

An alternative method for simulating particle suspensions using lattice Boltzmann

Luís Orlando Emerich dos Santos

Center of Mobility Engineering, Federal University of Santa Catarina,
88040-900, Florianópolis, Santa Catarina, Brazil

E-mail: emerich@lmpf.ufsc.br

Paulo Cesar Philippi

Mechanical Engineering Department, Federal University of Santa Catarina,
88040-900, Florianópolis, Santa Catarina, Brazil

E-mail: philippi@lmpf.ufsc.br

Abstract. In this study, we propose an alternative way to simulate particle suspensions using the lattice Boltzmann method. The main idea is to impose the non-slip boundary condition in the lattice sites located on the particle boundaries. The focus on the lattice sites, instead of the links between them, as done in the more used methods, represents a great simplification in the algorithm. A fully description of the method will be presented, in addition to simulations comparing the proposed method with other methods and, also, with experimental results.

Keywords: Lattice Boltzmann method, Particulate flow, Particle-fluid interactions

1. Introduction

Particulate flows are found in many industrial processes [1, 2, 3, 4], and have been subjected to considerable scientific investigation. Recently, computer simulations have become an effective tool in these studies and several methods have been applied, such as finite element method [5], Lagrange-multipliers [2, 3], direct forcing method [6], lattice Boltzmann methods [1, 4, 7, 8, 9, 10, 11, 12, 13, 14, 15, 16], solving the Stokes equation near the particles (Physalis) [17] and combining two or more methods [14, 18, 19].

In this study, we propose an alternative way to simulate suspensions using the lattice Boltzmann method. The main idea is to impose the non-slip boundary condition in the lattice sites representing the particle boundaries. The focus on lattice sites, instead of the link between them, as done in the more used methods [11], represents a great simplification in the algorithm. Similar approaches, focusing on the lattice sites were already tried [1], although without popularity due, probably, to difficulties several in the implementation.

Its important to mention that the simplifications we propose can reduce the accuracy in describing the details of the flow near the particles, and these details can or cannot

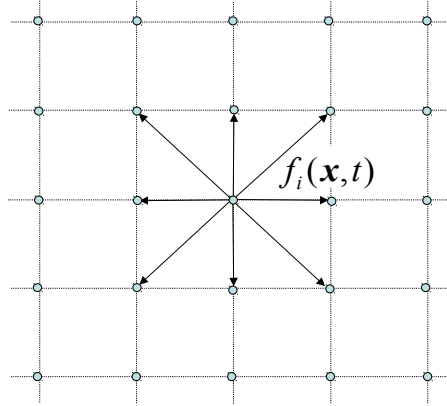


Figure 1. The D2Q9 lattice, used in two-dimensional simulations. The arrows represent the distributions $f_i(\mathbf{x}, t)$, and circles represent the lattice sites.

be important, depending on the problem one wants to simulate. In the simulations we have done until now, in spite of the simplifications, the results we obtain are similar to the results obtained by other methods (see section 3).

2. The model

In this section we introduce the lattice Boltzmann method and present the model describing the particle-fluid interaction. Interactions among particles and between a particle and a solid surface will also be discussed in this section.

2.1. The lattice Boltzmann model

The lattice-Boltzmann method (LBM) is based on the discretization of the Boltzmann's mesoscopic equation[20, 21, 22], usually with the BGK approach for the collision operator (for a comprehensive review see [23]). In the LBM scale, the system is described using a single particle distribution function, $f_i(\mathbf{x}, t)$, representing the number of particles with velocity \mathbf{c}_i at the site \mathbf{x} and time t , where $i = 0, \dots, b$. The particles are restricted to a discrete lattice, in a manner that each group of particles can move only in a finite number b of directions and with a limited number of velocities (see Fig. 1). Therefore, physical and velocity space are discretized. The local macroscopic properties such as total mass (the particle mass, m , is assumed unitary), $\rho(\mathbf{x}, t)$, and total momentum, $\rho(\mathbf{x}, t)\mathbf{u}(\mathbf{x}, t)$, can be obtained from the distribution function in the following way:

$$\rho(\mathbf{x}, t) = \sum_i f_i(\mathbf{x}, t), \quad (1)$$

$$\rho(\mathbf{x}, t)\mathbf{u}(\mathbf{x}, t) = \sum_i f_i(\mathbf{x}, t)\mathbf{c}_i. \quad (2)$$

The Lattice Boltzmann equation, that is, the discrete version of the Boltzmann equation with the BGK collision, operator is written

$$f_i(\mathbf{x} + \delta_i\mathbf{c}_i, t + \delta_t) - f_i(\mathbf{x}, t) = -\frac{\delta_t}{\tau} [f_i(\mathbf{x}, t) - f_i^{eq}(\rho, \mathbf{u})] \quad (3)$$

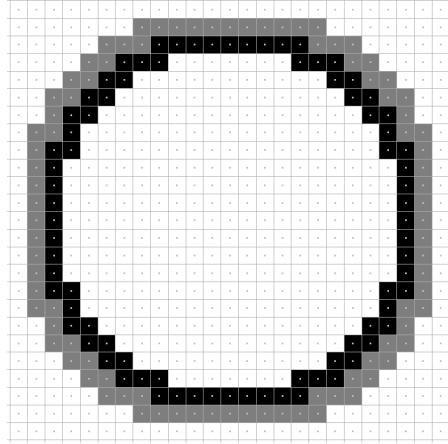


Figure 2. Boundary sites characterizing a particle. The boundary sites (BS) are depicted in dark gray and the internal sites (IS), in dark. The particle's boundary are regard to be between the IS and BS sites.

where, δ_t is the time step and $f_i^{eq}(\rho, \mathbf{u})$ is a polynomial approximation of the Maxwell-Boltzmann equilibrium distribution [24, 20, 21, 22], a function of the local variables $\rho(\mathbf{x}, t)$ and $\mathbf{u}(\mathbf{x}, t)$. It can be shown, through a Chapman-Enskog analysis, that this system macroscopically will evolve according to the Navier-Stokes equations with a kinematic viscosity given by

$$\nu = c_s^2 (\tau - 1/2), \quad (4)$$

where c_s is the sound velocity, a constant depending on the set of velocities \mathbf{c}_i .

2.2. Particle-fluid interaction

The basic idea of the method is that the fluid in contact with a solid surface must acquire the velocity of this surface, considering the non-slip condition. Keeping this in mind, a set of boundary sites can be used to describe the particle. This approach is similar to the one presented in [7] and [11], although we focus in the lattice sites and not in the links between them. We denote *boundary sites* (BS) the particle sites in contact with fluid, and *internal sites* (IS) the particle sites in contact with the boundary sites (see Fig.2). The particle's boundary is regarded to be halfway between the IS and the BS sites. A particle will be represented by its central position \mathbf{x}_p , a radius r_p , a mass m_p and a moment of inertia I_p . Its velocity will be denoted \mathbf{u}_p , and the angular velocity $\boldsymbol{\omega}_p$. Only spherical particles will be considered.

The presence of a particle will be represented only by its effects on the fluid in contact with the particle, altering the dynamics of the sites BS and IS. The position of these sites will be denoted by \mathbf{x}_B and \mathbf{x}_I , respectively, and its integer counterpart (or the nearest integer of each component of the vectors) by $[\mathbf{x}_B]$ and $[\mathbf{x}_I]$, respectively. Velocities and densities in the sites $[\mathbf{x}_B]$ and $[\mathbf{x}_I]$ will be denoted \mathbf{u}_B , \mathbf{u}_I and ρ_B , ρ_I . We emphasize that all sites will be updated by the usual collision/propagation steps, but the IS and BS sites, in addition to these steps, will be submitted to a set of substeps included between the collision and the propagation steps. These substeps are presented in the sequence.

- *Particle-fluid momentum transfer*

This substep is executed only in the BS sites. As was previously mentioned, the velocity in the BS sites must acquire the particle's velocity. This velocity, considering the angular velocity, is

$$\mathbf{u}'_B = \mathbf{u}_p + (\mathbf{x}_B - \mathbf{x}_p) \times \boldsymbol{\omega}_p. \quad (5)$$

To impose this velocity in the fluid, that is in lattice sites, the equilibrium distribution is employed, setting $f_i([\mathbf{x}_B], t) = f_i^{eq}(\rho, \mathbf{u}'_B)$.

Naming $\mathbf{p}_B = \rho_B \mathbf{u}_B$ the linear momentum of a BS site, we compute

$$\Delta \mathbf{p}_B = \rho_B (\mathbf{u}'_B - \mathbf{u}_B), \quad (6)$$

and

$$\Delta \mathbf{l}_B = \rho_B (\mathbf{x}_B - \mathbf{x}_p) \times (\mathbf{u}'_B - \mathbf{u}_B), \quad (7)$$

where $\Delta \mathbf{l}_B$ represents the change in the angular momentum caused by the change in the linear momentum $\Delta \mathbf{p}_B$.

Finishing this step we have the total momentum exchanged, $\Delta \mathbf{P}_B$ and $\Delta \mathbf{L}_B$:

$$\Delta \mathbf{P}_B = \sum_{BS} \Delta \mathbf{p}_B \quad (8)$$

$$\Delta \mathbf{L}_B = \sum_{BS} \Delta \mathbf{l}_B \quad (9)$$

- *Particle's acceleration*

This substep accounts for the change in particles velocity caused by fluid. According to the Newton's third law of motion, we simply compute

$$\mathbf{u}'_p = \mathbf{u}_p - \Delta \mathbf{P}_B / m_p, \quad (10)$$

$$\boldsymbol{\omega}'_p = \boldsymbol{\omega}_p - \Delta \mathbf{L}_B / I_p, \quad (11)$$

$$\mathbf{u}'_I = \mathbf{u}'_p + (\mathbf{x}_I - \mathbf{x}_p) \times \boldsymbol{\omega}'_p. \quad (12)$$

- *Updating of particle's position*

Due to the spherical symmetry it is not necessary to take into account the rotation of the particles. The position is updated by doing:

$$\mathbf{x}'_p = \mathbf{x}_p + \delta_t \mathbf{u}'_p. \quad (13)$$

The positions of boundary and internal sites, also, must be updated:

$$\mathbf{x}'_B = \mathbf{x}_B + \delta_t \mathbf{u}'_p; \quad (14)$$

$$\mathbf{x}'_I = \mathbf{x}_I + \delta_t \mathbf{u}'_p. \quad (15)$$

Clearly, this procedure includes errors of order (δ_t^2) , more precise procedures could be employed. Nevertheless, there is a lot of imprecision in describing the shape of the particle, therefore it is not necessary to be so precise in updating particle's position.

- *Velocity of the internal sites*

To impose this velocity the equilibrium distribution is employed again, setting $f_i([\mathbf{x}'_I], t) = f_i^{eq}(\rho, \mathbf{u}'_I)$.

Some comments are necessary to clarify the physics behind these sub-steps. Consider a particule that is found with a velocity \mathbf{u}_p different of the fluid velocity around it, in the beginning of the particle–fluid interaction step. This situation never occurs in the continuum but this is possible in discrete models due to the discretization of time. Particle and fluid must then exchange linear and angular momentum until the fluid around the particle acquires the velocity of the particle surface. In this process the particle velocity also changes due to the fluid reaction on the particle and in accordance with Newton’s third law of motion. Action and reaction happen simultaneously in the physical process, but in the discrete case this occurs in steps 1 and 2. In the first step the particle transfers linear and angular momentum to the fluid. In consequence the fluid in contact with the particle surface particle accelerates until have acquired the same particle velocity. As it was earlier mentioned two hypotheses are used for this step: non-slipping on the particle surface and the hypotheses that the fluid-particle equilibration takes a time interval smaller than the time step used in the simulation. This enables the use of an equilibrium distribution to impose the velocities. With the fluid velocity altered, we then calculate the change in the linear and angular momentum of the fluid due to this acceleration. These variations must be the same as the corresponding changes for the particle, in accordance with the Newton’s third law. We then proceed to step 2 and recalculate the particle velocity. The velocity to be imposed in sites IS is also calculated in accordance with the new particle velocity.

In a third step, the position of the particle and sites IS and BS are changed. The spherical symmetry of the particles eases this step since only the translation velocities are taken into account in the calculation of the new positions. It must be stressed that although sites BS belong to the fluid phase, they have their position changed in accordance with the particle velocity. Indeed, these sites are in the particle boundary and must follow its displacement. In other words the displacement of the boundary sites is independent of the fluid particles that are occupying these sites, in a given instant.

Finally, in a fourth step, we impose the velocity \mathbf{u}'_I to the sites IS. This step is important because during the propagation step the information in these sites is transferred to the adjacent sites BS. Therefore, the sites BS will have their velocity composed by the particle and fluid velocities and will define a new change of momentum in the following time step.

2.3. Interaction between particles

Especially in simulations involving a great number of particles, as the simulation presented in subsection 3.4, the interaction between particles must carefully be addressed. There are many techniques to treat these interactions, possibly the most popular approach is to introduce a repulsive force between particles when the gap between becomes smaller than a given threshold[14]. We chose another approach in this work, treating the collisions as occurring between completely rigid particles (hard-core collisions). In this way it is not necessary to set the parameters of repulsive forces. We simply impose (see Fig.3)

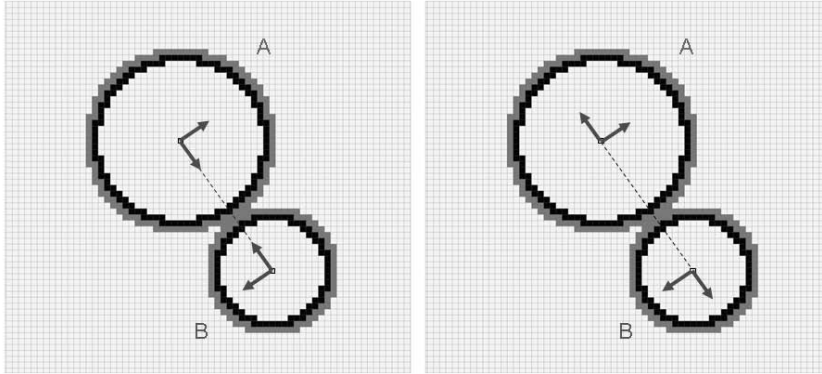


Figure 3. Collision between two particles, A and B. The arrows indicate the normal and tangential velocities before and after the collision. The velocities are represented in the center of mass reference frame.

$$\mathbf{v}'_{An} = -\mathbf{v}_{An}, \quad (16)$$

$$\mathbf{v}'_{Bn} = -\mathbf{v}_{Bn}, \quad (17)$$

$$\mathbf{v}'_{At} = \mathbf{v}_{At}, \quad (18)$$

$$\mathbf{v}'_{Bt} = \mathbf{v}_{Bt}, \quad (19)$$

where all velocities are represented in the center of mass reference frame. This imposition must be done before updating particles' positions, that is, it can be considered as part of the particle's acceleration substep.

It's necessary to underline that the way we chose to introduce the particle-particle interaction is not new, nor regarded as part of the method. Moreover, this choice was done considering solely the easeness in the implementation. In accordance with the Reynolds number, volume fraction of the particles and the involved force, more elaborated techniques, employing lubrication[8] or spring forces[25] may reveal to be necessary.

3. Validation

Four cases are presented in order to validate the model. The first case simulated was the flow around a massive two-dimensional particle. The particle's mass was chosen in such way that it doesn't move, therefore it's possible to compare the flow around the two dimensional particle and the flow around a solid cylinder, simulated using bounce-back. The drag coefficient for a massive particle was also computed considering several Reynolds number and compared with drag coefficients obtained by other methods. The second case simulated was the flow of a neutrally buoyant two-dimensional particle in a shear flow, the results are compared with the results presented by Feng and Michaelides[14]. A simulation of a sphere settling in a closed box was done in order to validate the model in a three-dimensional simulation. The results obtained was compared with the ones presented by ten Cate et al.[26]. Finally, it was simulated the sedimentation of 504 two-dimensional particles in an enclosure.



Figure 4. Geometry used to simulate the flow in a channel with an obstacle.

3.1. Flow around a massive two dimensional particle

The first geometry used to simulate the flow around a massive particle is depicted in Fig. 4. The simulations of a flow around a solid cylinder was carried out using bounce-back boundary conditions and the simulation of flow around a massive particle was done using the method proposed in this work, that is, using the equilibrium distribution to impose the velocities in the boundaries of the particle. The results of both simulations are presented in Fig. 5. To emphasize the deviations we plot in Fig. 6 the magnitude of the difference between the velocities. In the enclosed regions of Fig. 6 the deviations are of order 10^{-4} (the velocities in the simulations varying from zero to 0.075). It is important to notice that, in spite of deviations that can appear near the solid surface as result of applying different boundary conditions, the overall flow behavior is the same. Of course, depending on the applications one intends to focus, these differences must be taken into account.

Simulations to obtain drag coefficients were also carried out in the geometry presented in Fig. 7. Velocities varying from 0.00417 to 0.1667 in the x direction were imposed at the boundaries (left, right, top and bottom), resulting in the Reynolds number varying from $Re = 1$ to $Re = 40$. The results obtained are shown in Fig. 8, beside the results published by Rajani et al.[27] and Silva et al. [28]. Although the drag coefficients computed in this work were systematically lower than the results obtained by other methods, the importance of these errors is dependent on what we want to describe in a given problem, as it can be seen in the simulations presented in the sequence.

3.2. Neutrally buoyant two dimensional particle in a shear flow

The motion of a neutrally buoyant two-dimensional particle moving in viscous fluid was already simulated using LBM [29],[30],[14] as well as using finite element method [5], and was chosen as one of the validations of the present model. The geometry of the problem is described in Fig. 9, where $U_w/2$ and $-U_w/2$ are the velocities imposed. Periodic boundary conditions are imposed in the left and right boundaries. The relaxation time was set $\tau = 0.6$, which implies a kinematic viscosity $\nu = 1/30$, in lattice units. The parameters chosen are the same used in Feng & Michaelides paper[14], in order to ease the comparison. The velocity equals $U_w/2 = 1/120$, therefore, the shear rate for the flow is $\gamma = U_w/H = 1/120$, and a dimensionless time, t^* , is defined $t^* = t\gamma^2 r_s/\nu$, where r_s is the particle radius. Fig. 10, shows the migration of the particle, initially at the position $y = H/4$, toward the center. The

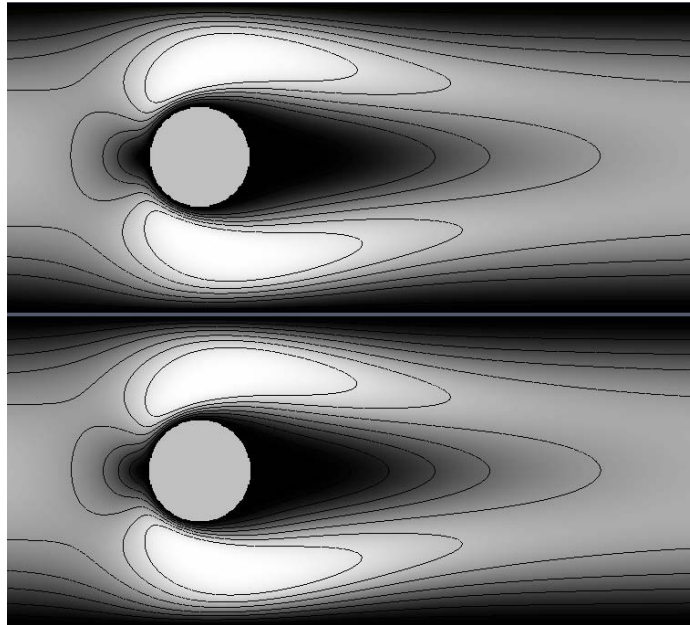


Figure 5. Top: flow around a solid cylinder. Bottom: flow around a massive particle. The velocities vary from zero (black) to 0.075 (white)

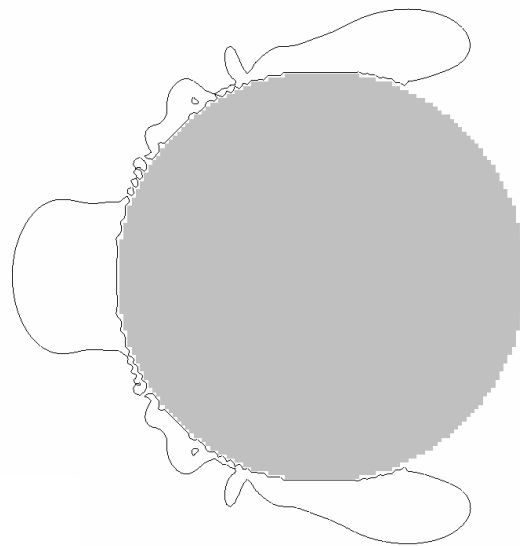


Figure 6. The difference in the velocities considering the simulations using a solid cylinder and a massive particle. In the enclosed region the errors are of order $O(10^{-4})$, outside the errors are smaller than this.

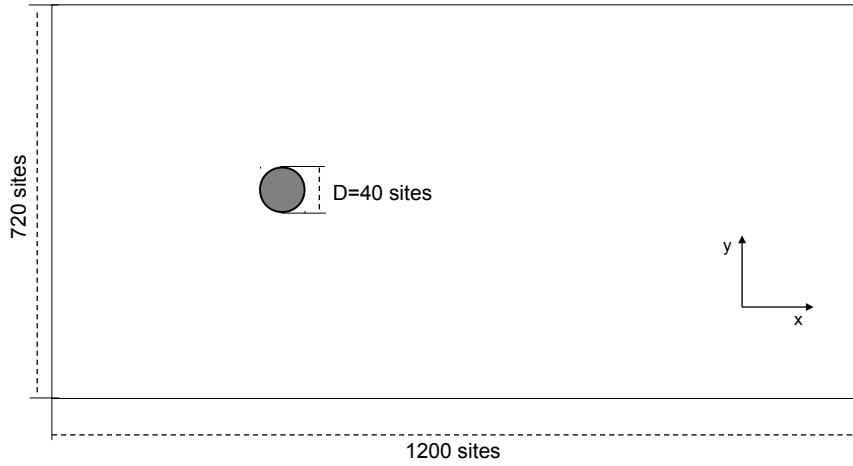


Figure 7. The geometry used to compute the drag coefficient of the 2D particle.

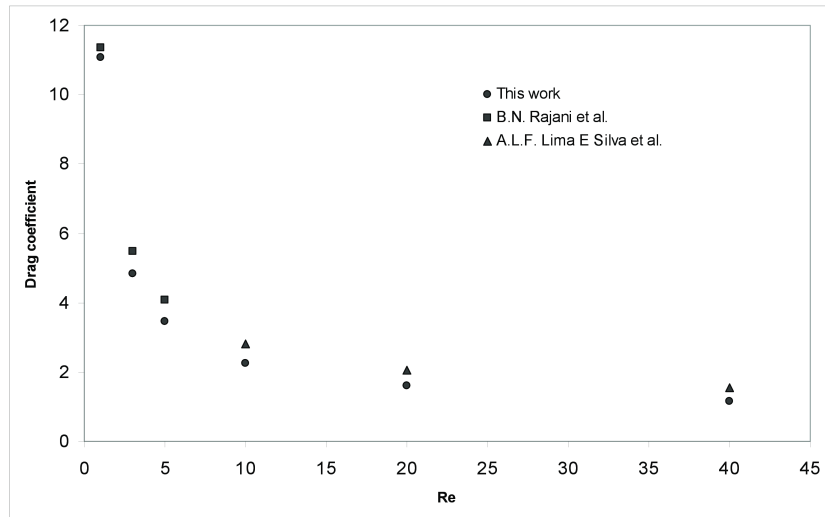


Figure 8. Drag coefficients for Reynolds number varying from one to forty. The results computed using the proposed model are compared with the work by Rajani et al. [27] (Reynolds from one to five) and Silva et al. [28] (Reynolds from ten to forty).

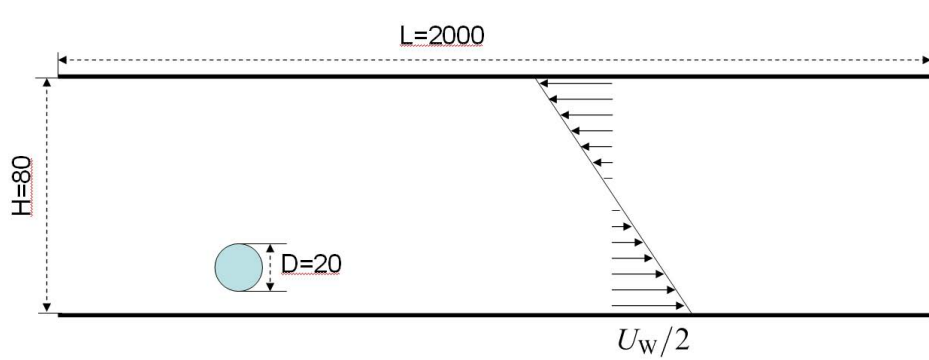


Figure 9. Schematic depiction of the problem simulated: a neutrally buoyant two dimensional particle in a shear flow

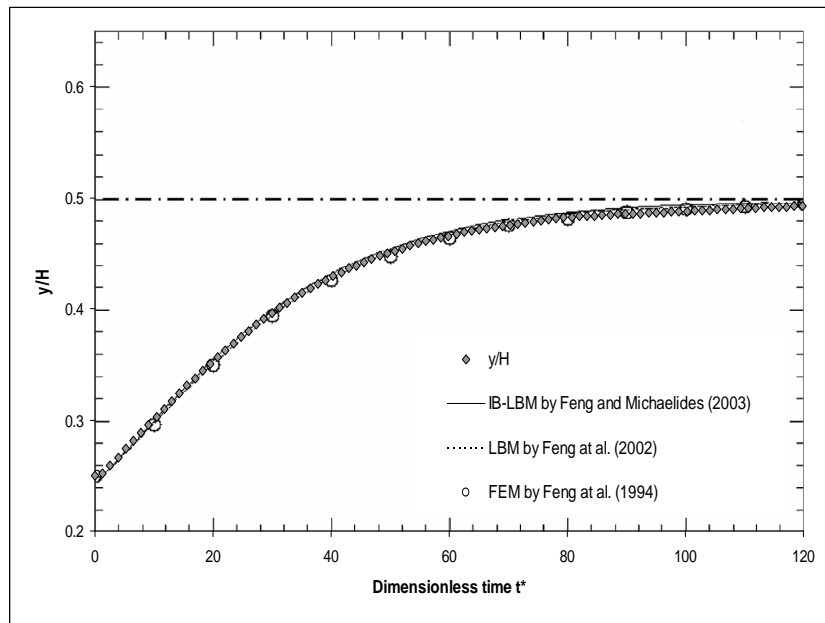


Figure 10. A neutrally buoyant particle in a shear flow – comparison of the results obtained using the proposed model for fluid-solid interaction and previous models. The y-axis shows the particle's position with respect to the lateral of channel divided it's width H.

agreement between the results using the proposed model and the previous models are quite good.

3.3. A sphere settling in a closed box

In this subsection the trajectory and velocity of a sphere settling in a closed box is simulated using the model here proposed and compared with experimental results obtained by Cate et al. [26]. The settling sphere has a diameter of $D = 15mm$ and density $\rho = 1120kg/m^3$. The container dimensions are depth \times width \times height=

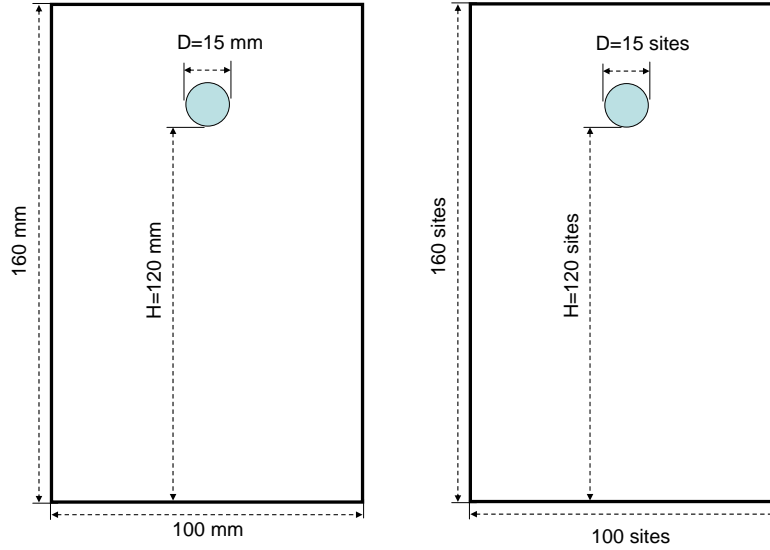


Figure 11. Schematic depiction of the geometry used in the experiments (left) and in the simulations (right).

$100 \times 100 \times 160\text{mm}$ (see Fig. 11). Four cases were simulated considering the different densities and viscosities of the fluid in which the sphere will settle, corresponding to a Reynolds number varying from $Re = 1.5$ to $Re = 32.2$. The fluid characteristics and the parameters used in the simulations are shown in Table 1.

Table 1. Fluid properties in the experiment and parameters used in simulations.

	$\rho_f[\text{kg}/\text{m}^3]$	$\mu_f[10^{-3}\text{Ns}/\text{m}^2]$	τ	$\delta_t[10^{-3}\text{s}]$
Case E1	970	373	0.9	0.347
Case E2	965	212	0.9	0.607
Case E3	962	113	0.8	0.851
Case E4	960	58	0.9	2.207

Figure 12 and 13 present comparisons between simulation and experiment for the trajectories and velocities of the settling particle, respectively.

3.4. 504 particles settling in a closed box

The problem of a large number of particles settling in a closed 2D box was already simulated by other methods [2], [14]. All the parameters were chosen in order to compare with the previous works. That is, 504 circular particles with diameter $D = 0.625\text{cm}$ settling in box having 10^{-2}m width and 10^{-2}m height. The fluid and particle densities are $\rho_f = 1000\text{kg}/\text{m}^3$ and $\rho_p = 1010\text{kg}/\text{m}^3$, respectively, and the fluid kinematic viscosity is $\nu_f = 10^{-6}\text{m}^2/\text{s}$. Representing the box by 512×512 sites and using a relaxation time $\tau = 0.9915$ we will have a time step of 0.00025s . The process of sedimentation simulated from the initial state to 24s is presented in

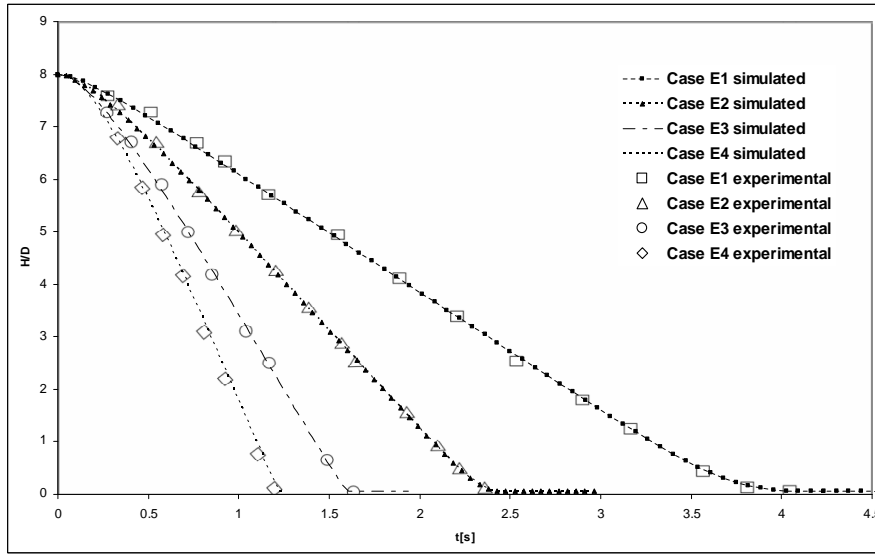


Figure 12. The position of the particle settling in a closed box. The simulated results are compared with the experimental results from Cate et al. (2002). The y-axis presents particle's position H (see Fig. 11), divided by its diameter D . The x-axis shows time in seconds.

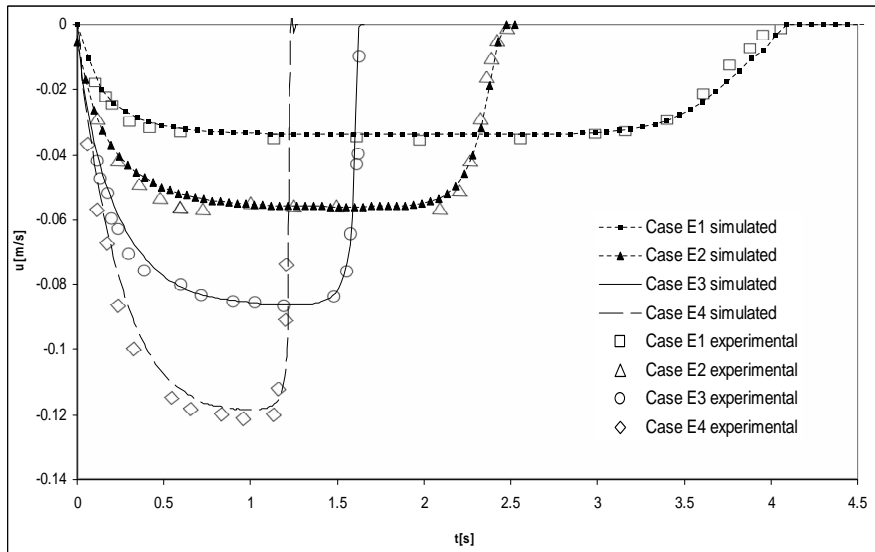


Figure 13. Comparison between simulation and the experimental results from Cate et al. (2002). The y-axis shows the velocity of the settling particle in meters per second and the x-axis indicates time in seconds.

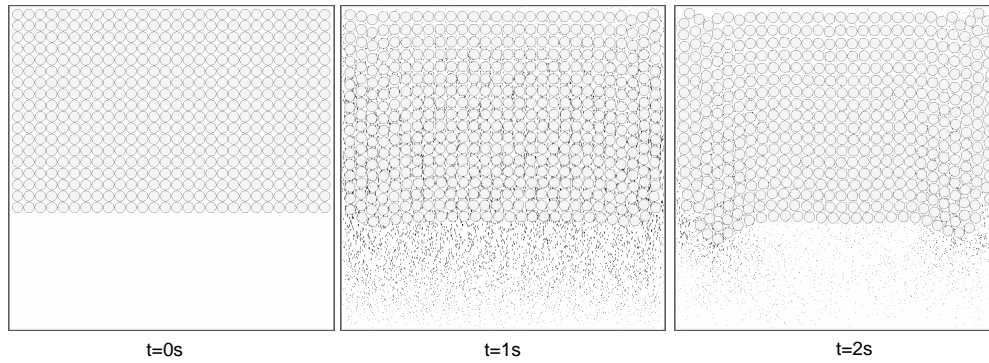


Figure 14. Configurations of the settling particles.

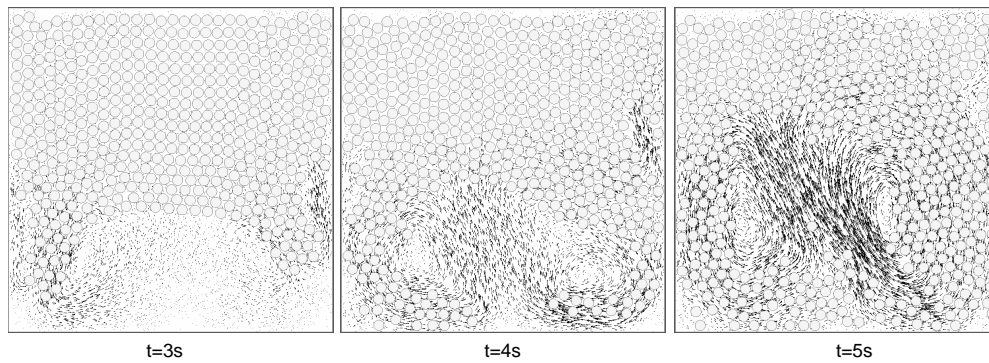


Figure 15. Configurations of the settling particles.

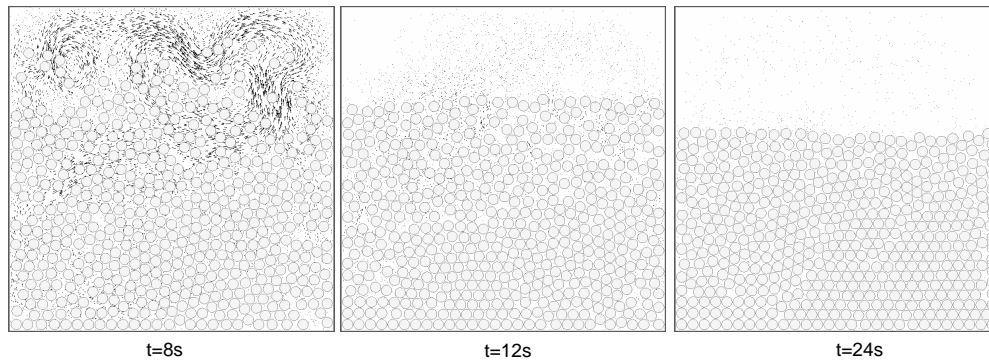


Figure 16. Configurations of the settling particles.

Fig. 14, Fig. 15 and Fig. 16. The figures show the development of a Rayleigh–Taylor instability and are, qualitatively, in agreement with the previous works. The differences between the three simulations (the one presented here and the simulations of refs. [2] and [14]) are, possibly, a result of the differences in treating the collisions between particles and differences arising from compressibility effects that are present in the lattice Boltzmann methods.

4. Conclusion

In this study an alternative and simpler way to simulate particle-fluid interactions is proposed. The lattice Boltzmann method is employed to simulate the fluid flow and the particles are simulated using the Newton's law. The coupling is made applying the equilibrium distribution function to assure the non-slip condition near the solid surfaces. Several simulations are presented showing that the method can simulate particle-fluid interactions with a precision comparable with other methods.

References

- [1] O. Behrend, "Solid-fluid boundaries in particle suspension simulations via the lattice boltzmann method," *Physical Review E* **52**, pp. 1164–1175, 1995.
- [2] R. Glowinski, T. W. Pan, T. I. Hesla, and D. D. Joseph, "A distributed lagrange multiplier/fictitious domain method for particulate flows," *International Journal of Multiphase Flow* **25**, pp. 755–794, 1999.
- [3] N. Patankar, P. Singh, D. Joseph, R. Glowinski, and T. W. Pan, "A new formulation of the distributed lagrange multiplier/ fictitious domain method for particulate flows," *International Journal of Multiphase Flow* **26**, pp. 1509–1524, 2000.
- [4] E.-J. Ding and C. K. Aidun, "Extension of the lattice-boltzmann method for direct simulation of suspended particles near contact," *Journal of Statistical Physics* **112**, pp. 685–708, August 2003.
- [5] J. Feng, H. H. Hu, and D. D. Joseph, "Direct simulation of initial-value problems for the motion of solid bodies in a newtonian fluid .2. couette and poiseuille flows," *Journal of Fluid Mechanics* **277**, pp. 271–301, 1994.
- [6] Z. Yu and X. Shao, "A direct-forcing fictitious domain method for particulate flows," *Journal of Computational Physics* **227**, pp. 292–314, 2007.
- [7] A. Ladd, "Numerical simulation of particulate suspension via a discretized boltzmann-equation .1. theoretical foundation," *Journal of Fluid Mechanics* **271**, pp. 285–309, 1994.
- [8] A. Ladd, "Numerical simulation of particulate suspension via a discretized boltzmann-equation .2. numerical results," *Journal of Fluid Mechanics* **271**, pp. 311–339, 1994.
- [9] C. Aidun and Y. Lu, "Lattice boltzmann simulation of solid particles suspended in a fluid," *Journal of Statistical Physics* **81**, pp. 49–59, 1995.
- [10] C. Aidun, Y. Lu, and E.-J. Ding, "Direct analysis of particulate suspensions with inertia using the discrete boltzmann equation," *Journal of Fluid Mechanics* **373**, pp. 287–311, 1998.
- [11] A. J. C. Ladd and R. Verberg, "Lattice-boltzmann simulations of particle-fluid suspensions," *Journal of Statistical Physics* **104**, pp. 1191–1251, September 2001.
- [12] B. Chopard and S. Marconi, "Lattice boltzmann solid particles in a lattice boltzmann fluid," *Journal of Statistical Physics* **107**, pp. 23–37, April 2002.
- [13] N.-Q. Nguyen and A. J. C. Ladd, "Lubrication corrections for lattice-boltzmann simulations of particle suspensions," *Physical Review E* **66**, p. 046708, 2002.
- [14] Z.-G. Feng and E. E. Michaelides, "The immersed boundary-lattice boltzmann method for solving fluid-particles interaction problems," *Journal of Computational Physics* **195**, pp. 602–628, 2004.
- [15] N.-Q. Nguyen and A. J. C. Ladd, "Sedimentation of hard-sphere suspensions at low reynolds number," *Journal of Fluid Mechanics* **525**, pp. 73–104, 2005.
- [16] J. Kromkamp, D. van den Ende, D. Kandhai, R. van der Sman, and R. Boom, "Lattice boltzmann simulation of 2d and 3d non-brownian suspensions in couette flow," *Chemical Engineering Science* **61**, pp. 858–873, 2006.
- [17] Z. Zhang and A. Prosperetti, "A second-order method for three-dimensional particle simulation," *Journal of Computational Physics* **210**, pp. 292–324, 2005.
- [18] Z.-G. Feng and E. E. Michaelides, "Proteus: a direct forcing method in the simulations of particulate flows," *Journal of Computational Physics* **202**, pp. 20–51, 2005.
- [19] Z. Wang, J. Fan, and K. Luo, "Combined multi-direct forcing and immersed boundary method for simulating flows with moving particles," *International Journal of Multiphase Flow* **34**(3), pp. 283–302, 2008.
- [20] X. He and L. Luo, "A priori derivation of the lattice boltzmann equation," *Physical Review E* **55**(6), pp. R6333–R6336, 1997.

- [21] X. Shan, X.-F. Yuan, and H. Chen, “Kinetic theory representation of hydrodynamics: a way beyond navier-stokes equation,” *Journal of Fluid Mechanics* **550**, pp. 413–441, 2006.
- [22] P. C. Philippi, L. A. Hegele, L. O. E. dos Santos, and R. Surmas, “From the continuous to the lattice boltzmann equation: The discretization problem and thermal models,” *Physical Review E* **73**(5), p. 056702, 2006.
- [23] S. Succi, *The Lattice Boltzmann Equation for Fluid Dynamics and Beyond*, Oxford University Press, 2001.
- [24] T. Abe, “Derivation of the lattice boltzmann method by means of the discrete ordinate method for the boltzmann equation,” *Journal of Computational Physics* **131**(1), pp. 241–246, 1997.
- [25] K. Höfler and S. Schwarzer, “Navier-stokes simulation with constraint forces: Finite-difference method for particle-laden flows and complex geometries,” *Physical Review E* **61**(6), pp. 7146–7160, 2000.
- [26] A. ten Cate, C. H. Nieuwstad, J. J. Derksen, and H. E. A. V. den Akker, “Particle imaging velocimetry experiments and lattice-boltzmann simulations on a single sphere settling under gravity,” *Physics of Fluids* **14**, pp. 4012–4025, November 2002.
- [27] B. Rajani, A. Kandasamy, and S. Majumdar, “Numerical simulation of laminar flow past a circular cylinder,” *Applied Mathematical Modelling* **33**, pp. 1228–1247, 2009.
- [28] A. L. E. Silva, A. Silveira-Neto, and J. Damasceno, “Numerical simulation of two-dimensional flows over a circular cylinder using the immersed boundary method,” *Journal of Computational Physics* **189**, pp. 351–370, 2003.
- [29] Z.-G. Feng and E. E. Michaelides, “Hydrodynamic force on spheres in cylindrical and prismatic enclosures,” *International Journal of Multiphase Flow* **28**, pp. 479–496, 2002.
- [30] Z.-G. Feng and E. E. Michaelides, “Interparticle forces and lift on a particle attached to a solid boundary in suspension flow,” *Physics of Fluids* **14**, pp. 49–60, January 2002.